ABA-C_{15}: A New Dye for Probing Solvent Relaxation in Phospholipid Bilayers

Jan Sýkora,[†] Virima Mudogo,[†,‡] Rudi Hutterer,[§] Miloš Nepras,[∥] Jozef Vaněrka,[∥] Petr Kapusta,[⊥] Vlastimil Fidler,[⊥] and Martin Hof*[,†]

J. Heyrovský Institute of Physical Chemistry, Academy of Sciences of the Czech Republic and Center for Complex Molecular Systems and Biomolecules, Cz-18223 Prague 8, Czech Republic, University of Kinshasa, P. O. Box 202, Kinshasa XI, Democratic Republic of Congo, Institute of Analytical Chemistry, Chemo- and Biosensors, University of Regensburg, D-93040 Regensburg, Germany, Department of Technology of Organic Compounds, University of Pardubice, Cz-53210 Pardubice, Czech Republic, and Department of Physical Electronics, Czech Technical University in Prague, Cz-18000 Prague 8, Czech Republic

Received August 20, 2002. In Final Form: September 23, 2002

We synthesized and studied N-palmitoyl-3-aminobenzanthrone (ABA-C_{15}), which we proved to be an advantageous new fluorescent phospholipid membrane label. While the absorption of ABA-C_{15} in protic solvents shows negative solvatochromism, its fluorescence emission is substantially red-shifted when the polarity of the solvent is increased. ABA-C_{15} is excitable by lasers emitting in the range between 390 and 490 nm; it exhibits reasonable quantum yields in protic solvents and binds with high affinity to small unilamellar phospholipid vesicles. Absorption, steady state fluorescence, and solvent relaxation data indicate that the aminobenzanthrone chromophore is located in the headgroup region of phospholipid bilayers in the liquid crystalline state of small unilamellar vesicles. The solvent relaxation kinetics probed by ABA-C_{15} in the liquid crystalline state is characterized by three solvent relaxation times in the order of 0.05, 0.2, and 1.5 ns, respectively. We observed that the relative contribution of the 0.05 ns component and the overall Stokes shift became larger with increasing difference between the experimental temperature and the main phase transition temperature; this suggests that the chromophore becomes more accessible by water molecules. In the gel phase, a component faster than 30 ps significantly contributes to the solvent relaxation kinetics. However, the solvent relaxation on the nanosecond time scale appears to be slower than in the liquid crystalline phase. The shape and time evolution of the time-resolved emission spectra suggest that two distinct microenvironments of the dye might be responsible for the atypical solvent relaxation characteristics in the gel phase.

Introduction

Solvent relaxation (SR) refers to the dynamic process of solvent reorganization in response to an abrupt change in charge distribution of a dye via electronic excitation. The temporal response can be monitored through the observation of the dynamic Stokes' shift $\nu(t)$ of the dye's emission maximum frequency. The complete time-dependent Stokes' shift $\Delta\nu$ ($\Delta\nu = \nu(0) - \nu(\infty)$) increases with increasing solvent polarity. Linear proportionality between $\Delta\nu$ and a dielectric measure of the solvent polarity has been verified experimentally.[1] Provided that this proportionality has been characterized for a certain probe, the determination of $\Delta\nu$ may yield quantitative information on the polarity of the probed microenvironment. At ambient temperatures, a typical relaxation process $C(t)$ ($C(t) = (\nu(t) - \nu(\infty))/\Delta\nu$) in an isotropic polar solvent starts with a fast inertial motion on the 0.05−0.5 ps time range, followed by rotational and translational diffusion occurring on the pico- to subnanosecond time scale.[1] In pure water, an (integral) average SR time (τ_r), defined as $\langle\tau_r\rangle \equiv \int_0^\infty C(t)\,dt$, of about 0.3 ps has been determined.[2]

On the other hand, it has been demonstrated[3,4] that a substantial part of the SR monitored by dyes associated with phospholipid bilayers occurs on the nanosecond time scale. Within the last 10 years, SR studies in bilayers became motivated 2-fold: First, a series of publications appeared demonstrating the benefit of this technique in detecting physiological relevant changes in the phospholipid bilayer organization.[5−9] The SR technique has been shown to detect "microviscosity" (τ_r) and "micropolarity" ($\Delta\nu$) changes in the bilayer due to temperature,[5,7,8] ethanol addition,[9] membrane curvature,[5] and variations in lipid composition[6−9] as well as due to the binding of calcium ions[6,8] and blood coagulation proteins.[8] The dyes used in those studies have been shown to be well-located within the hydrophobic backbone or the hydrophilic headgroup regions of the bilayer and were based on 2-amino-substituted naphthalene[4,5,7−9] and anthracene-9-carboxylic acid.[4,6] However, the absorption maxima of those dyes

* To whom correspondence should be addressed. E-mail: hof@jh-inst.cas.cz.

[†] Academy of Sciences of the Czech Republic and Center for Complex Molecular Systems and Biomolecules.

[‡] University of Kinshasa.

[§] University of Regensburg.

[∥] University of Pardubice.

[⊥] Czech Technical University in Prague.

(1) Horng, M. L.; Gardecki, J. A.; Papazyan, A.; Maroncelli, M. *J. Phys. Chem.* **1995**, *99*, 17311−17337.

(2) Jimenez, R.; Fleming, G. R.; Kumar, P. V.; Maroncelli, M. *Nature* **1994**, *369*, 471−473.

(3) Easter, J. H.; Brand, L. *Biochem. Biophys. Res. Commun.* **1973**, *52*, 1086−1092.

(4) Sýkora, J.; Kapusta, P.; Fidler, V.; Hof, M. *Langmuir* **2002**, *18*, 571−574.

(5) Hof, M.; Hutterer, R.; Perez, N.; Ruf, H.; Schneider, F. W. *Biophys. Chem.* **1994**, *52*, 165−72.

(6) Hutterer, R.; Schneider, F. W.; Lanig, H.; Hof, M. *Biochim. Biophys. Acta* **1997**, *1323*, 195−207.

(7) Hutterer, R.; Schneider, F. W.; Hof M. *J. Fluoresc.* **1997**, *7*, 27−33.

(8) Hutterer, R.; Schneider, F. W.; Hermens, W. T.; Wagenvoord, R.; Hof, M. *Biochim. Biophys. Acta* **1998**, *1414*, 155−164 and refs 12, 13, 15, and 29 therein.

(9) Hutterer, R.; Hof, M. *Z. Phys Chem.* **2002**, *216*, 333−346.

10.1021/la026435c CCC: $22.00
Published on Web 10/26/2002

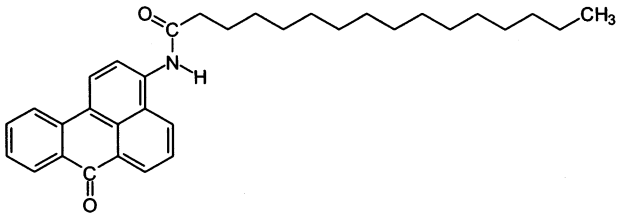

Figure 1. Structure of ABA-C_{15}.

range between 350 and 380 nm making them inaccessible for presently available pulsed picosecond diode lasers.[10] Subsequently, to those contributions demonstrating the benefit of the SR technique in biomembrane studies, studies addressing the question on the origin of slow relaxation components probed in lipid membranes were published.[11] It is proposed that ionic headgroups make the nearest water molecules nearly immobile and that those "bound" water molecules undergo slow exchange with "unbound" water molecules. While this sounds plausible, it only considers the role of the water molecules but not the influence of the charged headgroups on the SR kinetics. The influence of the chemical structure of the phospholipid headgroups on the SR monitored in the headgroup region of the bilayer has been demonstrated.[8]

As the number of SR probes commercially available so far is rather low, we engaged in the development of new membrane labels that would combine defined probe localization with a large change in charge distribution upon electronic excitation. N-Palmitoyl-3-aminobenzanthrone (ABA-C_{15}; Figure 1) is an example of such chromophore, and it presents some properties, the combination of which makes ABA-C_{15} uniquely suited to phospholipid membrane studies. In the present work, we report on its synthesis, on the photophysical properties of ABA-C_{15} in various solvents, on the incorporation of this compound in small unilamellar vesicles (SUV) characterized by fluorescence correlation spectroscopy (FCS), and on the steady state fluorescence characteristic of ABA-C_{15} incorporated in 1,2-dipalmitoyl-sn-glycero-3-phosphocholine (DPPC) SUV at different temperatures. The focus of this study, however, is the characterization of the dipolar SR probed by ABA-C_{15} in SUV composed of DPPC, 1,2-dimyristoyl-sn-glycero-3-phosphocholine (DMPC), and 1,2-dioleoyl-sn-glycero-3-phosphocholine (DOPC) at 27 °C using blue diode laser excitation ($\lambda_{exc} = 403.5$ nm; 150 ps full width at half-maximum (fwhm) of the pulse).

Materials and Methods

Synthesis, Isolation, and Characterization of ABA-C_{15}. The reaction scheme is shown in Figure 2. 3-Nitrobenzanthrone was prepared by nitration of benzanthrone with 87% HNO_3 in nitrobenzene at 50 °C for 2 h. The reaction mixture was cooled and diluted with ethanol. The precipitated crude product was filtered, washed with ethanol, and crystallized from acetic acid. 3-Aminobenzanthrone was prepared by reduction of 3-nitrobenzanthrone in a solution of sodium sulfide in water. Under stirring, the reaction mixture was heated and kept boiling for 2 h. The crude product was washed with hot water, dried, and crystallized from 80% ethanol. In the last step, 3-aminobenzanthrone was dissolved in acetone and triethylamine was added. Then, the acetone solution of palmitoyl chloride was added stepwise. The precipitated product was filtered and washed with acetone, diluted HCl, water, and with acetone again. The purity of all substances was checked by thin-layer chromatography, and their

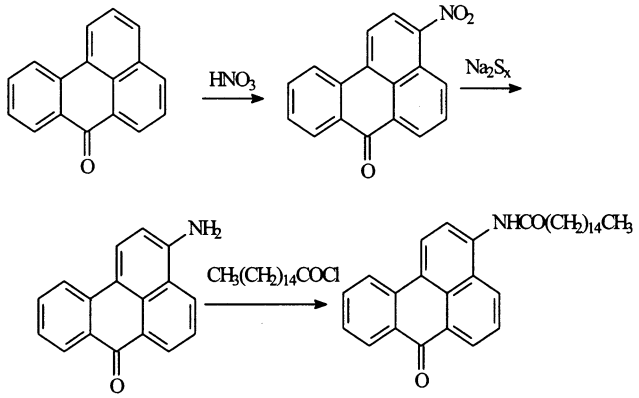

Figure 2. Reaction scheme for the preparation of ABA-C_{15}.

structure was confirmed by elemental analysis and mass spectrometry (data not sown).

Preparation of SUV. DPPC, DMPC, DOPC, and egg-phospha-tidylcholine (PC) were supplied by Avanti Lipids. The preparation of SUV from the turbid suspension of lipids in 50 mM Tris-100 mM NaCl buffer, pH 7.4, by sonication was performed as described previously.[4−8]

Steady State and Time-Resolved Fluorescence Measurements as Well as Absorption Measurements. Fluorescence decays and spectra were recorded with modified Edinburgh Instruments FSFL900 time-correlated single photon counting equipment. Decay kinetics were recorded by using blue laser diode IBH NanoLED-07 excitation source (403.5 nm peak wavelength, 150 ps fwhm of the pulse, 1 MHz repetition rate) and a cooled Hamamatsu R3809U-50 microchannel plate photomultiplier attached to Jobin-Yvon HR10 monochromator set to 8 nm resolution, all that providing the overall experimental time resolution of 30 ps. In all of the bulk fluorescence measurements, the used lipid-to-dye ratio was 100:1 with a total used lipid concentration of 0.2 mM. Absorption spectra have been recorded on a Perkin-Elmer Lambda 19 spectrometer. For the absorption measurements, a higher lipid-to-dye ratio (70:1) was used with a total used lipid concentration of 0.5 mM. The absorption, excitation, and emission spectra of ABA-C_{15} in polar and nonpolar (*n*-heptane) solvents were recorded at the concentrations of 5 and 10 μM, respectively. In all experiments, the temperature was controlled within ±0.5 °C with a water-circulating thermostat bath.

Time-Resolved Emission Spectra (TRES) and Time-Zero Spectrum. The primary data consist of a set of emission decays recorded at a series of wavelength spanning the steady state emission spectrum. The TRES are obtained by spectral reconstruction, which is a relative normalization of the fitted decays to the steady state emission spectrum. Log-normal fitting of TRES yields various characteristic parameters, such as fwhm and emission maxima ($\nu(t)$) of TRES.[1,4,8] The maxima of the estimated time-zero spectrum $\nu(t_0)$ were determined by the method described by Fee and Maroncelli.[12] As already shown,[12] very similar results as obtained by this method for a maximum of a time-zero spectrum $\nu(t_0)$ in an environment of interest can be obtained simply by subtraction of the difference (in cm^{-1}) between the maxima of the absorption and emission spectra recorded in nonpolar reference solvent from the value of the maximum of the absorption spectrum of the dye recorded in the system of interest.

FCS. FCS measurements were carried out using a fluorescence correlation spectrometer "ConfoCor 1", manufactured by Carl Zeiss Jena. ConfoCor 1 is an Ar^+ laser-adapted AXIOVERT 135 TV microscope with a 100/100 binocular phototubus. The air-cooled Ar^+ laser supplies the excitation wavelength of 488 nm. The obtained autocorrelation function $G(\tau)$, where τ represents the delay time, was fitted with the model function for the three-dimensional translation diffusion in an ellipsoid volume. The concentration of the lipid and the dye used were 0.2 mM and 0.02 μM, respectively, corresponding to a lipid-to-dye ratio of 10 000:

(10) An overview of presently commercially available diode lasers may give two URL links: http://www.picoquant.com/_lightsources.htm or http://www.ibh.co.uk/products/sources.htm.

(11) Bhattacharyya, K.; Bagchi, B. *J. Phys. Chem. A* **2000**, *104*, 10603−10613 and ref 51 therein.

(12) Fee, R. S.; Maroncelli, M. *Chem. Phys.* **1994**, *183*, 235−247.

Table 1. Maxima of Absorption (ν_{abs}) and Emission Fluorescence (ν_{fl}) Spectra in Various Solvents and Vesicle Systems[a]

solvent	ν_{abs} (cm^{-1})	ν_{fl} (cm^{-1})[b]	solvent	ν_{abs} (cm^{-1})	ν_{fl} (cm^{-1})[b]
heptane[c]	22 920	19 600	cyclohexanol	23 400	17 700
methanol	23 890	17 260	DOPC	23 620	17 390
ethanol	23 770	17 420	DMPC	23 450	17 670
propanol	23 590	17 510	DPPC	23 210	17 860
butanol	23 480	17 570			

[a] The samples were thermostated at 27 °C. [b] The emission maximum is recorded by setting the excitation monochromator to the maximum of absorption. [c] For the reasons discussed in the text, the excitation spectrum was used instead of the absorption spectrum.

1. For further details concerning this setup and data analysis, please consult ref 13.

Results and Discussion

Photophysical Properties of ABA-C_{15} in Various Solvents. The position of the absorption maxima of ABA-C_{15} has been determined in a series of nonprotic, nonaromatic solvents (complete data set not shown). The obtained values range from 23 810 cm^{-1} for the most polar representative acetonitrile (the value of reaction field factor F is 0.305; F is a simple measure of solvent polarity and is defined as $F = (\epsilon_r - 1)/(2\epsilon_r + 1) - (n_D^2 - 1)/(2n_D^2 + 1)$, where ϵ_r and n_D are the dielectric constant and optical refractive index of the solvent, respectively) to 23 440 cm^{-1} for dibutyl ether ($F = 0.096$) with medium to low solvent polarity. It appears that higher solvent polarity leads to a blue shift in the absorption maxima. However, we have found several deviations from this trend (e.g., 23 390 cm^{-1} for dimethyl sulfoxide ($F = 0.263$)). Thus, we cannot claim a general negative solvatochromism in the absorption within nonprotic, nonaromatic solvents.

This picture changes when examining the dependence of absorption maxima on the solvent polarity within a series of aliphatic alcohols (Table 1). These solvents certainly model to some extent the situation of a chromophore located in certain domains of a phospholipid/water system. The absorption spectra are continuously blue-shifted by increasing the solvent polarity, clearly indicating negative solvatochromism. The absorption maximum of ABA-C_{15} in the most polar alcohol methanol ($F = 0.309$) is at 23 890 cm^{-1}, whereas in cyclohexanol ($F = 0.235$) it appears at 23 400 cm^{-1}. The fluorescence in those alcohols shows positive solvatochromism: the fluorescence emission maximum shifts continuously from 17 700 cm^{-1} in cyclohexanol to 17 260 cm^{-1} in methanol. When detecting the fluorescence intensity at the individual emission maxima, the excitation spectra appear to be identical to the corresponding recorded absorption spectra.

The determination of the absorption spectrum of ABA-C_{15} in nonpolar solvents such as *n*-heptane is complicated by its low solubility in such solvents. A low extinction at apparent micromolar dye concentration prevents a precise determination of the position of the absorption maximum. When increasing the dye concentration, on the other hand, the absorption spectrum significantly broadens comprising the appearance of a blue-shifted shoulder, possibly indicating the formation of aggregates. However, at an apparent dye concentration of approximately 10 μM in *n*-heptane, the sample shows a reasonable fluorescence spectrum with an emission maximum at 19 600 cm^{-1}. Setting the emission monochromator to the latter value, the excitation scan reveals a well-resolved excitation spectrum with its maximum at 22 920 cm^{-1}.

To obtain information about the position of the time-zero spectrum and the corresponding $\nu(t_0)$ values in protic solvents, we have recorded steady state emission spectra in an ethanol/methanol (1:1) mixture at 77 K. This solvent mixture is known to form transparent glass at the given temperature.[14] It has been shown that under those conditions the solvation dynamics is much slower than nanosecond fluorescence decay times[15] and thus the steady state emission spectrum might serve as an approximation of the time-zero spectrum.[12] The emission spectrum in the glass exhibits a substantial vibrational structure. To compare the position of the recorded emission spectrum below the glass transition temperature with the unstructured fluorescence spectrum in the nonpolar solvent heptane, and thus in absence of dielectric SR, we make use of the midpoint wavenumber $\nu_{md} = 0.5\ \nu_- + 0.5\ \nu_+$, where ν_- and ν_+ are the wavenumbers of the half-height points on the low (ν_-) and high (ν_+) frequency sides of the spectra. The obtained ν_{md} values of 19 820 and 19 450 cm^{-1} obtained for ABA-C_{15} in the ethanol/methanol glass and in *n*-heptane, respectively, give further evidence for the negative solvatochromism in the position of the Franck−Condon state and consequently in the absorption.

In summary, the fluorescence emission of ABA-C_{15} is substantially red-shifted when increasing the polarity of the solvent. The dye exhibits reasonable quantum yields[15] in protic solvents and is excitable by lasers emitting in the range between 390 and 490 nm. Thus, the spectral properties of the aminobenzanthrone chromophore fulfill the requirements for probing SR and allow the excitation by "rather inexpensive"[16] blue diode lasers with picosecond time resolution.[10]

Incorporation of ABA-C_{15} in SUV Observed by FCS. The new dye ABA-C_{15} can only be applied properly in membrane studies, if it can be assumed that the fluorescence originates exclusively from membrane-bound dyes under the used experimental conditions. To exclude a fluorescence contribution from dyes in the bulk water, we made use of the fact that ABA-C_{15} can be excited by an Ar^+ laser (488 nm) and performed fluorescence correlation experiments[13] on SUV consisting of DOPC. Lipid and dye concentrations were 0.2 mM and 0.02 μM, respectively. The obtained correlation function (Figure 3) was fitted satisfactorily with a one component fit. The fit to a model with two diffusing species yielded two components with identical diffusion coefficients, clearly excluding the existence of a second fluorescent species with different molecular weight. The obtained diffusion coefficient ($6.1 \pm 1.0 \times 10^{-12}$ m s^{-2}) is in a good agreement with previously published results[13] for sonicated SUV, ensuring that the entire fluorescence is from membrane-bound ABA-C_{15}. The FCS result clearly demonstrates that ABA-C_{15} binds with high affinity to SUV. Moreover, they show that ABA-C_{15} is an appropriate dye for single molecule studies.

Absorption and Steady State Fluorescence Characteristics of ABA-C_{15} When Incorporated in SUV. The absorption and fluorescence maxima of ABA-C_{15} in

(13) Beneš, M.; Billy, D.; Hermens, W. T.; Hof, M. *Biol. Chem.* **2002**, *383*, 337−341.

(14) Suppan, P.; Ghoneim, N. *Solvatochromism*, 1st ed.; Royal Society of Chemistry: London, 1997.

(15) The fluorescence lifetime of ABA-C_{15} in methanol, 2-propanol, acetonitrile, and dibutyl ether at 27 °C has been determined to be 8.6, 9.3, 10.3, and 1.9 ns, respectively. The fluorescence quantum yield of ABA-C_{15} in methanol, 2-propanol, acetonitrile, and dibutyl ether at 27 °C has been determined to be 0.33, 0.49, 0.59, and 0.07, respectively.

(16) By the term "rather inexpensive" we mean the affordable price of the blue diode lasers in comparison to the Ti−sapphire lasers. Moreover, the diode lasers are much easier to use.

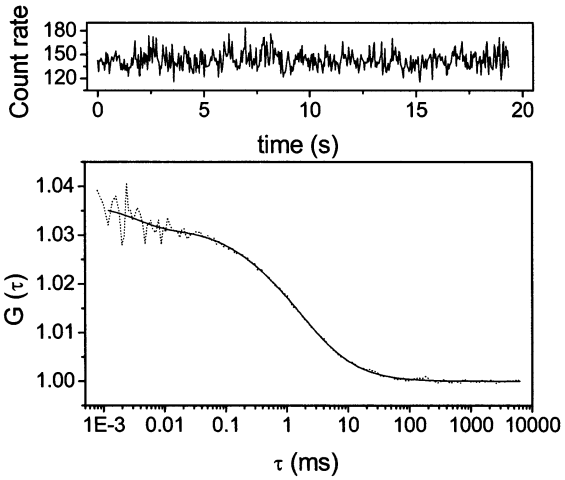

Figure 3. Typical results obtained by FCS for ABA-C_{15} incorporated in DOPC SUV. The upper plot illustrates the fluorescence signal as a function of time, and the bottom plot gives the correlation function (dotted curve) and the fit to the model function for the three-dimensional translation diffusion of a single species in an ellipsoid volume (solid curve). For further details concerning data analysis, please consult ref 13. The measurements have been performed at room temperature.

SUV composed of DPPC, DMPC, and DOPC at 27 °C are listed in Table 1. Comparison with the absorption maxima observed in alcohols indicated that the chromophore senses a polarity roughly comparable to a situation between *n*-propanol and *n*-ethanol or *n*-butanol and *n*-cyclohexanol for DOPC and DMPC, respectively. Because the emission maxima in these systems appear to be practically independent of the used excitation wavelength, the steady state fluorescence emission maxima may be used as well for a rather qualitative estimation of the polarity of the probed environment. The comparison of the corresponding steady state fluorescence emission maxima supports qualitatively the conclusions drawn by the comparison of the absorption maxima. The absorption maximum recorded in DPPC vesicles indicates that the chromophore probes an environment of lower polarity than cyclohexanol. In DPPC, we observe a small but significant red edge excitation shift (160 cm^{-1}; red edge excitation spectra were carried out at the emission wavelengths of 470, 480, 490, 495, and 500 nm). The appearance of such a red edge excitation shift might indicate that when the system is excited at its absorption maximum, the fluorescence originates to a significant extent from nonrelaxed states. Thus, we suggest to use the emission maximum observed for excitation at the red edge of the absorption spectrum as a rather qualitative indicator for the polarity of the dye environment. The emission maximum recorded at red edge excitation is located at 17 700 cm^{-1}, indicating a probed polarity similar to cyclohexanol. Mazeres et al. have used a distribution function of the dielectric constant plotted against the distance from the bilayer center to define the location of chromophores within the bilayer by using spectral data.[17] When using the same distribution function (see Figure 6 in ref 17) and the dielectric constants of the above compared alcohols, it can be concluded that the aminobenzanthrone chromophore is located within the headgroup region in all three investigated lipid systems. Moreover, it can be concluded that in the lipid system with the lower phase transition temperature T_m[18] the chromophore senses a microenvironment of higher polarity.

(17) Mazeres, S.; Schram, V.; Tocanne, J. F.; Lopez, A. *Biophys. J.* **1996**, *71*, 327−335.

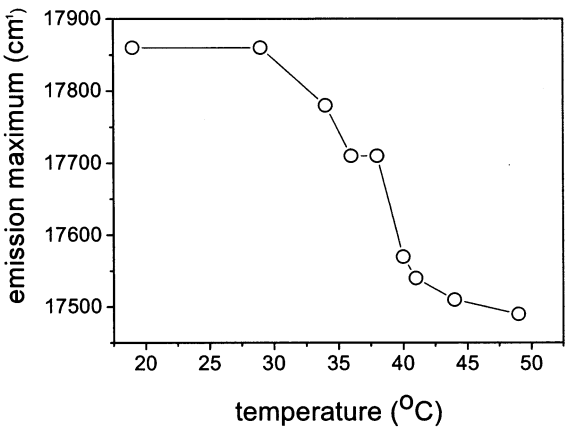

Figure 4. Dependence of position of fluorescence emission maxima of ABA-C_{15} on temperature in DPPC SUV. The excitation and emission wavelengths used were 415 and 560 nm, respectively.

Because we present in this contribution with ABA-C_{15} a new fluorescent membrane label, it is worth it to investigate the dependence of the position of the steady state fluorescence on the temperature and the phase state of the lipid. To this end, we have performed temperature scans of the position of the emission maximum in DPPC SUV, featuring a gel to liquid crystalline main phase transition approximately at 38 °C (Figure 4). Obviously, the fluorescence emission maximum of ABA-C_{15} gives quite precise information on the main transition in DPPC SUV.[18] It is interesting to compare the value of the fluorescence emission maxima listed in Table 1 with the DPPC transition curve. Apparently, the value for the midpoint of the DPPC transition curve corresponds roughly to the one found for DMPC at 27 °C. The two limiting values in Figure 4, on the other hand, correspond to DOPC and DPPC in Table 1. Although it is generally accepted that the main phase transition temperature for DMPC is slightly lower than 27 °C,[18] this result might indicate that under the given experimental conditions we probe coexisting gel and liquid crystalline DMPC domains.

Dipolar SR Probed by ABA-C_{15} in SUV Composed of DPPC, DMPC, and DOPC. The presented absorption and fluorescence data indicate that ABA-C_{15} might be suitable for probing SR in phospholipid bilayers. To verify this assumption, we have investigated steady state and time-resolved fluorescence characteristics of the dye incorporated in SUV composed of various lipid systems, mainly DPPC, DMPC, and DOPC. Moreover, we use these data to reveal the effect of different phase states on the solvation dynamics probed by ABA-C_{15} in those lipid systems.

A crucial point in bilayer studies remains the localization of the probe within the bilayer. Consulting the absorption and steady state fluorescence data, we have concluded that the chromophore of ABA-C_{15} should be located within the headgroup region of the bilayer of SUV. Further information on the relative probe localization might be gained by a comparison of the SR behavior probed by ABA-C_{15} with that probed by dyes with relatively well-known location. In a recent study, we have presented a comprehensive characterization of the SR behavior of seven (commercially available) membrane labels incorporated at different depth within phosphatidylcholine bilayers.

(18) The main phase transition temperatures for DOPC, DMPC, and DPPC in SUV are about −20, 22, and 38 °C, respectively (refs 21 and 22). Please note that there are practically no pretransitions in SUVs composed of those lipids (ref 22).

Table 2. Maxima of the Estimated Time-Zero Spectra $\nu(t_0)$ and the Total Stokes Shift $\Delta\nu(t_0 - t_{inf})^b$ for Three Investigated Lipid Systems[a]

	$\nu(t_0)$ (cm^{-1})	$\Delta\nu(t_0 - t_{inf})^b$ (cm^{-1})
DOPC	20 300	3030
DMPC	20 160	2660
DPPC	19 890	2260

[a] The data were recorded at 27 °C. [b] The value of total Stokes shift was generated as a difference between the maximum of the estimated time-zero spectrum ν (t_0) and the maximum of the spectrum ν (t_{inf}) obtained by spectral reconstruction at time 10 ns. At longer times than 10 ns after excitation, the TRES do not shift anymore in all three investigated systems.

The (integral) average SR times in PC SUV probed by the headgroup label 6-propionyl-2-dimethylaminonaphthalene (Prodan) and 6,8-difluoro-4-heptadecyl-7-hydroxycoumarin, which is believed to probe the external interface, have been determined to be 1.0 and 0.4 ns, respectively.[4] Using identical experimental conditions and analytical approaches as in the cited study,[4] we determined an (integral) average SR time probed by ABA-C_{15} in PC SUV of about 0.6 ns. The comparison of these results might suggest that the aminobenzanthrone chromophore probes the outermost region of the hydrophilic headgroup of PC bilayers.

To get a complete picture on any SR process, a precise knowledge about the emission spectrum of the Franck−Condon state is essential. The group of Maroncelli[1,12] showed that the frequency of the $t = 0$ peak emission, $\nu(t_0)$, of a chromophore in neat solvents can be calculated quite accurately when the absorption and fluorescence spectra in a nonpolar reference solvent, as well as the absorption spectrum in the system of interest, are known.[1,12] In a recent publication, we have adapted this approach for phospholipid bilayer systems, which enabled us to give a quantitative description of the SR process probed in the external interface, headgroup region, and hydrophilic backbone region in PC bilayers in the liquid crystalline phase.[4] In the case of ABA-C_{15}, however, its low solubility in nonpolar solvents prevented a precise determination of its absorption spectrum in a nonpolar reference solvent. For that reason, excitation spectra that can be scanned at lower concentrations than absorption spectra were recorded for a large range of solvents and were found practically identical to the absorption ones. Thus, it was assumed that the position of the peak maximum of the excitation spectra in neat solvents could serve as a valuable input parameter for the "t_0 estimation". Naturally, the obtained maxima of the estimated Franck−Condon spectra, $\nu(t_0)$, of ABA-C_{15} in SUV composed of DPPC, DMPC, and DOPC at 27 °C (Table 2) show the same trends as already discussed for the corresponding absorption spectra (Table 1). Considering the observed negative solvatochromism in the absorption and, consequently, in the Franck−Condon spectra, ABA-C_{15} again appears to probe the environment of highest polarity in DOPC bilayers, while the probed environment in DPPC appears to be lowest one.

It might be interesting to compare the listed $\nu(t_0)$ values with the fluorescence emission maximum obtained in the polar protic glass (ethanol/methanol 1:1). As discussed above, the vibrationally structured emission spectrum in ethanol/methanol glass is characterized by a midpoint wavenumber ν_{md} value of 19 820 cm^{-1} , which is lower than the maximum of the estimated time-zero spectrum $\nu(t_0)$ for the investigated lipid systems. On the first glance, this observation indicates a too low polarity in the case of the glass system. It is known that the dielectric constant of solvents is increasing by decreasing temperature. Thus, the comparison of the corresponding absorption maxima (Table 1) indicates that the polarity in the examined ethanol/methanol glass is certainly higher than the probed polarity in the lipid systems listed in Table 2. We can offer two possible explanations for this discrepancy: First, it has been shown that inhomogeneous fluorescence decay kinetics lead to time-dependent shifts of the fluorescence spectra of solvatochromic probe molecules in high-viscous and vitrified polar solvents.[19] Second, the midpoint wavenumber ν_{md} of a vibrationally structured fluorescence emission spectrum may not completely correspond to the maximum of an unstructured emission band.

To reconstruct TRES of ABA-C_{15} in the investigated lipid systems, the corresponding emission decays recorded at a series of wavelengths spanning the steady state emission spectrum have been recorded. At the blue edge of the fluorescence emission, generally four exponentional fits were needed to get satisfactory results. At longer wavelengths, the decay became less complex. The picosecond component (around 50 ps) disappeared, and even negative amplitudes were needed for fitting. This phenomenon is typical when observing solvation dynamics. Spectral reconstruction yields TRES, which can be characterized by their fwhm and emission maxima ($\nu(t)$). Because the spectral shape of the TRES, as well as the time evolution of the fwhm of ABA-C_{15}, significantly differ for probing DPPC SUV as compared with DOPC and DMPC SUV, we first discuss the latter two systems.

The shape of the TRES determined in DOPC and DMPC lipid systems is qualitatively similar to those found for other dyes probing the liquid crystalline phase of phospholipid bilayers[4,6−9] (Figure 5). The time evolution of the fwhm of the TRES follows the typical course characterized by its increase at shorter times reaching the maximum and further decrease at longer times (Figure 6). The appearance of such a fwhm profile indicates that the ensemble of fluorescing chromophores senses an environment of similar micropolarity and microviscosity and that a substantial part of SR process is captured with the instrumental setup available. The comparison of the $\Delta\nu$ values determined by using the $\nu(t_0)$ obtained by $t = 0$ estimation with those obtained exclusively by TRES reconstruction shows that at least 85% (Table 3) of the solvation dynamics is captured by the given time resolution of about 30 ps. This fact enables reliable fitting of correlation function $C(t)$ providing profound information on the kinetics of the solvation process. In the case of both DOPC and DMPC, three exponential fits were found satisfactory. This finding might be compared to a study of 6,8-difluoro-4-heptadecyl-7-hydroxycoumarin in PC bilayers, where also three components were needed for the characterization of the SR process.[4] The DOPC and the DMPC systems feature a component close to the time resolution of the experiment, a subnanosecond, and a nanosecond component on the order of 0.05, 0.20, and 1.5 ns, respectively. The relative contribution (see a_1 values in Table 3) of the 0.05 ns component differs significantly for DOPC and DMPC proposing a larger contribution of subnanosecond relaxation in DOPC vesicles. While the contribution and SR time of the 0.2 ns component are approximately equal, the slow part of SR differs in both fitted times and amplitudes. The results shown in Table 3 indicate that the SR process on the nanosecond time scale occurs significantly slower in DMPC vesicles as

(19) Fee, R. S.; Milsom, J. A.; Maroncelli, M. *J. Phys. Chem.* **1991**, *95*, 5170−5181.

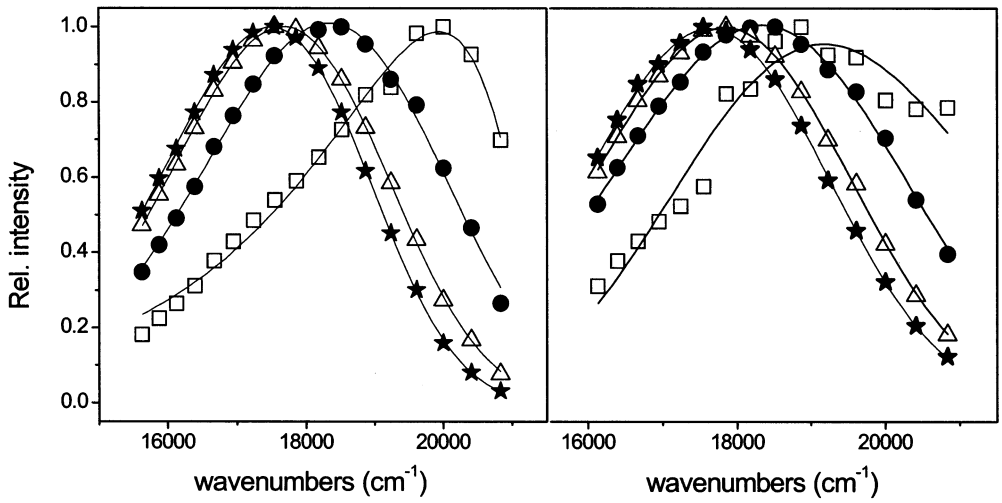

Figure 5. TRES of ABA-C_{15} in DMPC SUV (left panel) and DPPC SUV (right panel) reconstructed at different times after excitation (□, 0.0; ●, 0.5; △, 2.5; ★, 8.0 ns). Because the shapes of the TRES obtained for DOPC SUV are very similar to those obtained for DMPC SUV, they are not displayed. The experiments were carried out at 27 °C.

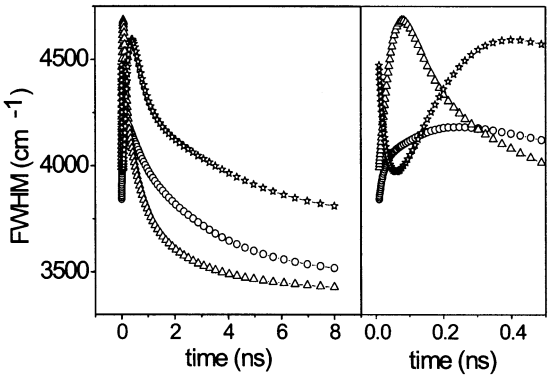

Figure 6. Time dependence of fwhm of the reconstructed TRES for DOPC (△), DMPC (○), and DPPC (☆) SUV. The right panel shows the fwhm profile for the first 0.5 ns after excitation. The data were recorded at 27 °C.

Table 3. SR Times τ_i[a], Relative Amplitudes a_i[a], and (Integral) Average SR Times[b] for Three Investigated Lipid Systems[d]

	τ_1 (ns) (a_1)	τ_2 (ns) (a_2)	τ_3 (ns) (a_3)	τ_r (ns)	% SR observed[c]
DOPC	0.05 (0.55)	0.21 (0.25)	1.40 (0.20)	0.39	84
DMPC	0.05 (0.40)	0.22 (0.19)	1.71 (0.41)	0.77	85
DPPC				0.89	64

[a] SR times t_i and relative amplitudes a_i were obtained by the multiexponentional fitting of $C(t)$:

$$C(t) = \sum_{i=1}^{3} a_i \exp(-t/t_i)$$

$C(t)$ for DPPC SUV was not fitted for the reasons mentioned in the text. [b] The (integral) average SR time t_r is defined as $\langle\tau_r\rangle \equiv \int_0^\infty C(t)\,dt$. [c] The % SR observed is obtained by comparison of the $\Delta\nu$ values determined by using the $\nu(t_0)$ with those obtained exclusively by TRES reconstruction. [d] All of the parameters described in the table were obtained from the data recorded at 27 °C.

compared to DOPC vesicles. This conclusion can be readily seen by visual inspection of $C(t)$ (Figure 7). Another important property obtained by TRES is the overall Stokes shift providing the information on micropolarity of the probe environment. The observed Stokes shift is larger for the DOPC lipid system (Table 2) confirming the above-discussed hypothesis that ABA-C_{15} is located in a more

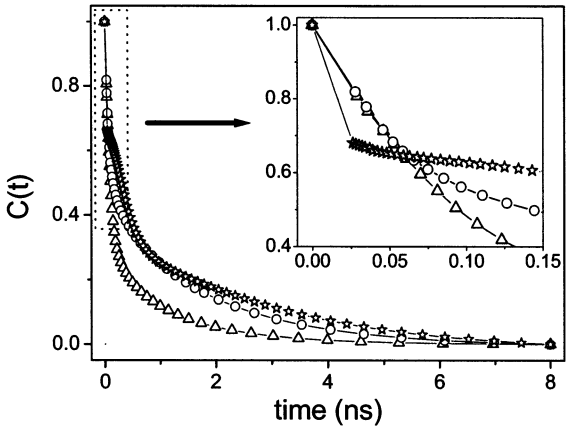

Figure 7. Correlation functions $C(t)$ for ABA-C_{15} in DOPC (△), DMPC (○), and DPPC (☆) vesicles at 27 °C. For DOPC and DMPC lipid systems, the multiexponential fits of $C(t)$ are shown, using the $\nu(t_0)$ obtained by the time-zero estimation. Because no satisfactory fit for the DPPC lipid system was obtained, raw data are displayed. The maximum $\nu(t_0)$ of estimated time-zero spectrum was used to gain the first point (time = 0 ns). The right panel shows the $C(t)$ profile for the first 0.15 ns after excitation.

polar environment far above the phase transition than close to the phase transition temperature. Moreover, the comparisons of the $\Delta\nu$ values and the values for the (integral) average SR time τ_r show that the SR above the main transition temperature occurs faster on average when probing a microenvironment of higher polarity. This trend has already been observed for various membrane labels.[4]

The behavior of ABA-C_{15} in DPPC vesicles differs significantly from the two previously described cases. The visual inspection of the appearance of TRES at short times after excitation (Figure 5) reveals a deviation from an emission spectrum of a single species.[1,7,8] The fwhm time dependence also shows deviations from the common profile[1,4,7,8] as an untypical decrease is observed at short times after excitation (Figure 6). These observations might be explained by the presence of a second microenvironment characterized by a SR process, which takes place far beyond our time resolution and only its very end is possible to detect. The fitting of the correlation function for DPPC appeared to be rather difficult due to the fact that only 64% (Table 3) of the SR process is captured by the time

resolution of the experiment. Thus, we omit fitting of the correlation function and use the (integral) average SR time (Table 3) for the description of the overall SR kinetics. The τ_r value was found to be somewhat larger in comparison to the lipid systems in the liquid crystalline phase. In contradiction to the trends observed for the DMPC and DOPC systems, the slower average SR time in the case of DPPC is paralleled by a significant increase of the contribution of a SR process, which occurs on a time scale faster than the time resolution of the experiment. This shift of a significant part of the SR to the picosecond time domain is paralleled by a slow solvation dynamics on the nanosecond time scale. This statement is easy to confirm by the visual inspection of correlation functions for all investigated lipid systems (Figure 7). Interestingly, the overall Stokes shift $\Delta\nu$ of ABA-C_{15} in DPPC vesicles exhibits the lowest value suggesting that the dye in DPPC vesicles is on average embedded in the least polar environment of all investigated lipid systems. We believe that our data for the first time give evidence that two dye localizations characterized by very different microviscosities may have to be discussed for the SR process in the gel phase probed by fluorescent headgroup labels.

In conclusion, it can be assumed that the solvation dynamics of ABA-C_{15} in SUV strongly depends on the phase state of a phospholipid bilayer. Above the phase transition temperature, the probed micropolarity and "microfluidity" follow the typical trend and become larger with an increasing difference between the experimental temperature and the main phase transition temperature. The fact that the relative contribution of the component close to the time resolution of the experiment and the overall Stokes shift $\Delta\nu$ are significantly larger for DOPC and DMPC might propose that in the first case the aminobenzanthrone chromophore is more accessible by water molecules. In the gel phase, an ultrafast component ($<$30 ps) is dominating the SR kinetics. On the other hand, the SR on the nanosecond time scale appears to be somewhat slower than in the liquid crystalline phase. When considering the shape and time evolution of the TRES, we suggest that two distinct microenvironments of the dye might be the origin for the observed untypical SR characteristics in the gel phase.

Conclusions

In view of the striking advantages of the newly developed blue laser diodes with simple handling and relatively low costs[10,16] providing picosecond pulses at MHz repetition rates, it is important to design membrane labels, which allow the application of such a diode laser. Within the past few years, we have shown that the SR technique is a valuable tool in membrane studies. In our opinion, there is no membrane label commercially available that allows both the use of those lasers and the sound interpretation[20] of the observed time-dependent Stokes shifts. In this paper, we present ABA-C_{15}, a new compound exhibiting reasonable quantum yields and large Stokes shifts. ABA-C_{15} appears to be located within the headgroup region of phospholipid bilayers in the liquid crystalline phase. We demonstrate that laser excitation of ABA-C_{15} at 404 nm as well as 488 nm makes SR and single molecule studies of phospholipid vesicles possible.

Acknowledgment. We thank the Ministry of Education, Youth and Sports of the Czech Republic (via LN 00A032 (J.S., V.M., M.N., J.V., and M.H.) and J04/98: 210000022 (P.K. and V.F.)) for financial support. We thank Mark Maroncelli for providing computer programs for the time-zero spectrum estimation.

LA026435C

(20) A major requirement for valid application or physical interpretation of SR studies in bilayers is the knowledge about the location of the used chromophore.

(21) Marsh, D. *Handbook of Lipid Bilayers*; CRC Press: Boca Raton, Florida, 1990.

(22) Koynova, R.; Caffrey, M. *Biochim. Biophys. Acta* **1998**, *1376*, 91−145.